Behavior of dry medium and loose sand-foundation system acted upon by impact loads

Adnan F. Ali[1a], Mohammed Y. Fattah[*2] and Balqees A. Ahmed[3b]

[1]*Civil Engineering Department, University of Baghdad, Baghdad, Iraq*
[2]*Building and Construction Engineering Department, University of Technology, Baghdad, Iraq*
[3]*Faculty Member, Civil Engineering Department, University of Baghdad, Baghdad, Iraq*

Abstract. The experimental study of the behavior of dry medium and loose sandy soil under the action of a single impulsive load is carried out. Different falling masses from different heights were conducted using the falling weight deflectometer (FWD) to provide the single pulse energy. The responses of soils were evaluated at different locations (vertically below the impact plate and horizontally away from it). These responses include; displacements, velocities, and accelerations that are developed due to the impact acting at top and different depth ratios within the soil using the falling weight deflectometer (FWD) and accelerometers (ARH-500A Waterproof, and Low capacity Acceleration Transducer) that are embedded in the soil and then recorded using the multi-recorder TMR-200. The behavior of medium and loose sandy soil was evaluated with different parameters, these are; footing embedment, depth ratios (D/B), diameter of the impact plate (B), and the applied energy. It was found that increasing footing embedment depth results in: amplitude of the force-time history increases by about 10-30%. due to increase in the degree of confinement with the increasing in the embedment, the displacement response of the soil will decrease by about 25-35% for loose sand, 35-40% for medium sand due to increase in the overburden pressure when the embedment depth increased. For surface foundation, the foundation is free to oscillate in vertical, horizontal and rocking modes. But, when embedding a footing, the surrounding soil restricts oscillation due to confinement which leads to increasing the natural frequency, moreover, soil density increases with depth because of compaction, that is, tendency to behave as a solid medium.

Keywords: dry; medium sand; loose sand; impact; embedment; response

1. Introduction

There are two types of forces/loads that may act on soil or the foundation of soil-structure interaction namely, static and dynamic loads. The differences between two types are inertial force (due to accelerated motion), damping, strain rate effect, and oscillation (stress reversals). Dynamic response of a soil can be caused by different loading conditions such as earthquake ground motion; wave action; blast; machine vibration; and traffic movement.

Machine foundations with impact loads are common powerful sources of industrial vibrations. These foundations are generally transferring vertical dynamic loads to the soil and generate ground vibrations which may harmfully affect the surrounding structures or buildings. Dynamic effects range from severe trouble of working conditions for some sensitive instruments or devices to visible structural damage (Svinkin 2008).

For a given size and geometry of the foundation, and the soil properties, the natural frequency of an embedded foundation will be higher and its amplitude of vibration will be smaller compared to a foundation resting on the surface.

Increasing the depth of embedment may be a very effective way in reducing the vibration amplitudes (Prakash and Puri 2006), same results was found by Al-Homoud and Al-Maaitah (1996), Mandal and Roychowdhury (2008), Al-Ameri, (2014), Bhandari and Sengupta (2014), Fattah *et al*. (2015).

Al-Homoud and Al-Maaitah (1996) tested many free and forced vertical vibrations models conducted on surface and embedded models for footings on dry and moist poorly graded sand. It was found that there is an increase in natural frequency and a reduction in amplitude with the increase in footing base area, same results was found by Kim *et al*. (2001), Fattah *et al*. (2014, 2016), Al-Ameri (2014).

Ergun *et al*. (2016) investigated the free vibration and buckling behaviors of hybrid composite beams having different span lengths and orientation angles subjected to different impact energy levels. The impact energies are applied in range from 10 J to 30 J. Free vibration and buckling behaviors of intact and impacted hybrid composite beams are compared with each other for different span lengths, orientation angles and impact levels. In free vibration analysis, the first three modes of hybrid beams are considered and natural frequencies are normalized. It was seen that first and second modes are mostly affected with increasing impact energy level. Also, the fundamental natural frequency is mostly affected with the usage of mold that have 40 mm span length (SP40). Moreover, as the impact energy increases, the normalized critical buckling

∗Corresponding author, Ph.D.
 E-mail: myf_1968@yahoo.com
[a]Professor
[b]Lecturer

Two rollers for adjusting the height

Sliding rail

Sand raining box

The falling weight deflectometer (FWD)

Wires connecting the accelerometer to the data logger
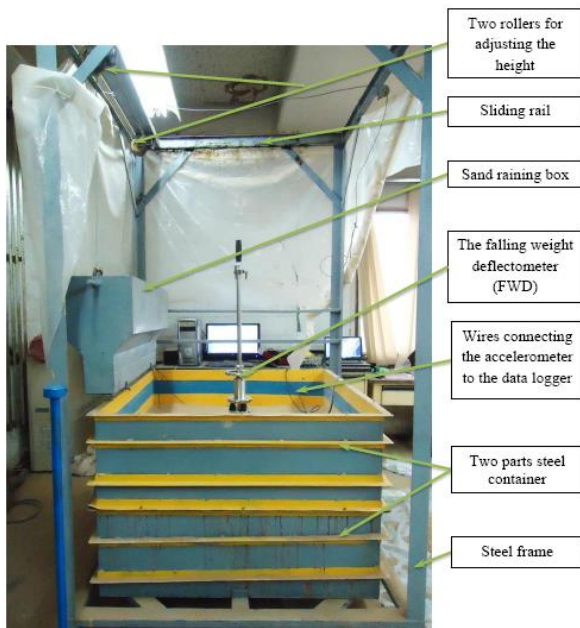
Two parts steel container

Steel frame

Fig. 1 The setup of the soil model

loads decrease gradually for 0o and 30o oriented hybrid beams but they fluctuate for the other beams

Nonlinear vibrations of an Euler-Bernoulli beam resting on a nonlinear elastic foundation were discussed by Fatih Karahan and Pakdemirli (2017). In search of approximate analytical solutions, the classical multiple scales (MS) and the multiple scales Lindstedt Poincare (MSLP) methods were used. The case of primary resonance was investigated. Amplitude and phase modulation equations were obtained. Steady state solutions were considered. Frequency response curves obtained by both methods were contrasted with each other with respect to the effect of various physical parameters. For weakly nonlinear systems, MS and MSLP solutions were in good agreement. For strong hardening nonlinearities, MSLP solutions exhibited the usual jump phenomena whereas MS solutions are not reliable producing backward curves which are unphysical.

The main objectives of this research are to predict soil behavior under impact loads. Emphasis will be made on attenuation of waves induced by impact loads through the soil. Conducting an experimental investigation on sandy soils was established to survey how to study the behavior of these soils under the effect of impact loads with different applied kinetic energy taking into account several factors: the embedment and diameter of the foundation, and the energy of the impact load.

2. Experimental work

A small scale model is implemented to simulate a physical model of a foundation resting on a dry or saturated soil media under impact load. The dynamic system is the soil medium through which waves propagate outward from sources of impact load. The input signal of the system is the impulse response of the ground at the place of installation of the foundation; the output signal is the dynamic response of a location of interest situated on a foundation receiving impulse or within the soil stratum. The tests were performed in dense soil state under impact load with different energy forces. Two footing sizes were adopted and the models were tested at the surface of the soil and at a depth of 0, 0.5B, B, and 2B (where B is the diameter of the footing).

2.1 Description of the soil model

Fig. 1 shows the setup that was used to carry out tests, it consists of a steel box with walls made of plates 2 mm thick and a base as a soil container, and the falling weight deflectometer (FWD) to apply impact loads on the soil model with a base bearing plate of two sizes which is dealt with as a shallow foundation on the soil under impact load. The steel box consists of two parts with dimensions; length of 1200 mm, width of 1200 mm and height of 800 mm. Each part has a height of 400 mm and strengthened from the outside with loops of 40 mm right angle 2 mm thick spaced at 1330 mm in the tangential direction.

The "raining technique and tamping" used to deposit the soil in the testing tank at a known and a uniform density was adopted in preparing the tested soil. The device consists of a steel hopper, with dimensions of (1200 mm in length, 300 mm in width and 450 mm in height) which is ended with an inclined funnel mounted above the testing tank and used as a hopper to pour the testing material from different heights through two rollers. In order to facilitate the horizontal movement of the steel tank, a simple sliding system was prepared for this purpose.

2.2 Measurement devices

The vertical impact load tests are conducted to simulate different impact loads using different falling masses (5 kg or 10 kg) with a dropping height of (500 mm). Two sizes of the base bearing plate were used; 100 mm and 150 mm.

Response of the soil under impact load was measured by installing four accelerometers; two in the vertical direction at depths equal to B and 2B where B is the diameter of the base bearing plate that was used in the test. Other two accelerometers were used in the horizontal direction at determined distances from the source of the impact load at B and 2B from the plate center and buried at a depth of 10 mm from the surface. Two pore water pressure transducers in the condition of saturation were installed in the vertical direction at depths of B and 2B.

The soil used for the model tests is clean sand, passing through sieve No. 10 and retaining on sieve No. 100. It was brought from Kerbelaa (Al-Ekhether region west of Baghdad in Iraq. The physical properties of the sand are presented in Table 1.

3. Sand preparation method and calibration

Raining technique were used to prepare the sand in the test tank. Table 2 shows the physical properties of the soil used in the tests. In order to achieve a uniform layer with a desired density, the raining technique was used to prepare the sandy soil model. This process was implemented using a

Table 1 Physical properties of the sand used

Property	Value	Unit	Standard of the test
Specific Gravity, Gs	2.65	----	ASTM D 854
Coefficient of gradation, C_c	0.79	----	ASTM D 422 and ASTM D 2487
Coefficient of uniformity, C_u	2.94	----	
USCS-soil type	SP	----	
Maximum dry unit weight, γ_{dmax}	17.8	kN/m^3	ASTM D 2049-69
Minimum dry unit weight, γ_{dmin}	14.9	kN/m^3	ASTM D4254-00
Maximum void ratio (e_{max})	0.7447	----	---------
Minimum void ratio (e_{min})	0.4605	----	---------

Table 2 Physical properties of the remolded sand used in the tests

Property	Value	Unit	Property
Medium state relative density, Dr, %	55.0	----	Medium state relative density, D_r, %
Loose state relative density, Dr, %	30.0	----	Loose state relative density, D_r, %
Dry unit weight in medium state	16.37	kN/m^3	Dry unit weight in medium state
Dry unit weight in loose state	15.66	kN/m^3	Dry unit weight in loose state
Void ratio at medium state	0.5881	----	Void ratio at medium state
Void ratio at loose state	0.6601	----	Void ratio at loose state

pre-manufactured steel hopper and steel tank through a repeated horizontal movement of the hopper which was controlled manually on the steel tank. The height of drop and the rate of discharge of the sand mainly affect the density of the sand layer in the raining method (Turner and Kulhawy 1987). Two rollers fixed at the top of the box were used to adjust the height of the raining device to control the height of the free fall of the sand. Several trials with different heights of fall were performed in order to achieve the desired relative density. In each trial, samples collected in small metal tins of known volumes positioned at several places in the test tank were used to check the density. After calculating the density, the void ratios of the sand and the relative density (Dr) as a function of the height of fall, the results are found. To prepare the loose state of sand with relative density of 30%, the height of the free fall will be 200 mm. After filling the raining box (tank) with sand and choosing the proper height of drop (200 mm), the sand was poured into the test tank. The soil layer was prepared in (6) layers with (10 cm) constant height for each one to attain the last elevation of (60 cm) from the bottom of container, and the same procedure is followed for preparing medium sandy soil with a relative density of 55% and choosing the suitable height for free fall of sand, which was 600 mm.

4. Impact test procedure
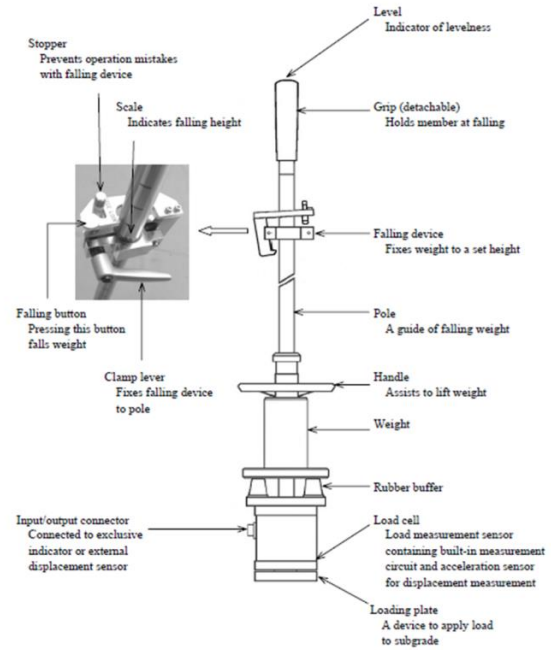
Fig. 2 Small FWD main body KFD-100A

Throughout this work, the falling weight deflectometer (FWD) was used to apply impact loads on the soil model. The small FWD system with the standard set with options Measurement/ Analysis Software TC-7100, additional weight (10 kg), and loading plate of 150 mm diameter were used. This equipment is capable of measuring the applied impact force-time history, displacement –time history at the soil surface, the modulus of elasticity of the soil, and the coefficient of subgrade reaction.

During each test, the acceleration-time history was measured at different depths utilizing accelerometers transducers (ARH-A waterproof, low capacity acceleration transducer (ARH-500A)) type. The basic structure of the FWD system consists of the main unit with built-in accelerometer (KFD-100A) and the indicator (TC-351F) as shown in Fig. 2. The indicator records the maximum load value, maximum displacement value and the analyzed coefficient of subgrade reaction and subgrade modulus. Various analysis results can be recorded and stored in the memory card. The data recorded in the memory card can be taken into a PC directly or via the indicator. The indicator system is capable of getting the reading every 0.05 msec. In addition, in this research, the load, acceleration, velocity, displacement waveform, O-P time (in case of load: time between the start point of loading and the maximum value point, in case of displacement: time between the start point of loading of displacement and the maximum value point of displacement), and time product are stored in the PC in addition to the analysis results from the indicator because the measurement/processing software (TC-7100) was used. This system drops the weight of the small FWD main body by free fall and measures the impact load and displacement using the load cell and the accelerometer. Displacement is measured by integrating the measurement value in the accelerometer twice. The measurement/processing software (TC-7100) is required for a measurement system that uses a
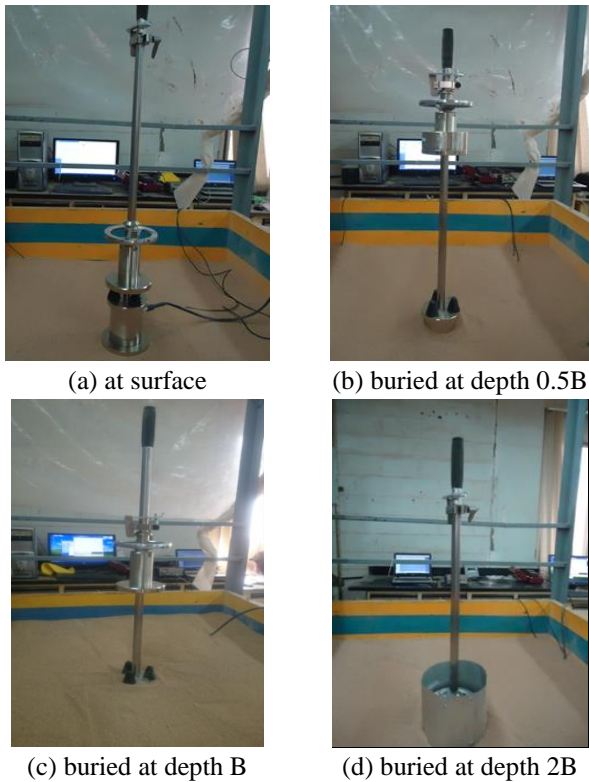
(a) at surface   (b) buried at depth 0.5B

(c) buried at depth B   (d) buried at depth 2B

Fig. 3 The state of impact load on the soil model

Table 3 Test designation adopted in the testing program

No.	Test designation	Soil density	Impact loading state	Size of bearing plate (mm)	The dropping mass (kg)
1	$L_SP_{10}M_5$	Loose	at surface	100	5
2	$L_{0.5b}P_{10}M_5$	Loose	at 0.5 B	100	5
3	$L_bP_{10}M_5$	Loose	at B	100	5
4	$L_{2b}P_{10}M_5$	Loose	at 2B	100	5
5	$M_SP_{10}M_5$	Medium	at surface	100	5
6	$M_{0.5b}P_{10}M_5$	Medium	at 0.5 B	100	5
7	$M_bP_{10}M_5$	Medium	at B	100	5
8	$M_{2b}P_{10}M_5$	Medium	at 2B	100	5
9	$L_SP_{15}M_5$	Loose	at surface	150	5
10	$L_{0.5b}P_{15}M_5$	Loose	at 0.5 B	150	5
11	$L_bP_{15}M_5$	Loose	at B	150	5
12	$L_{2b}P_{15}M_5$	Loose	at 2B	150	5
13	$M_SP_{15}M_5$	Medium	at surface	150	5
14	$M_{0.5b}P_{15}M_5$	Medium	at 0.5 B	150	5
15	$M_bP_{15}M_5$	Medium	at B	150	5
16	$M_{2b}P_{15}M_5$	Medium	at 2B	150	5
17	$L_SP_{10}M_{10}$	Loose	at surface	100	10
18	$L_{0.5b}P_{10}M_{10}$	Loose	at 0.5 B	100	10
19	$L_bP_{10}M_{10}$	Loose	at B	100	10
20	$L_{2b}P_{10}M_{10}$	Loose	at 2B	100	10
21	$M_SP_{10}M_{10}$	Medium	at surface	100	10
22	$M_{0.5b}P_{10}M_{10}$	Medium	at 0.5 B	100	10
23	$M_bP_{10}M_{10}$	Medium	at B	100	10
24	$M_{2b}P_{10}M_{10}$	Medium	at 2B	100	10
25	$L_SP_{15}M_{10}$	Loose	at surface	150	10
26	$L_{0.5b}P_{15}M_{10}$	Loose	at 0.5 B	150	10
27	$L_bP_{15}M_{10}$	Loose	at B	150	10
28	$L_{2b}P_{15}M_{10}$	Loose	at 2B	150	10
29	$M_SP_{15}M_{10}$	Medium	at surface	150	10
30	$M_{0.5b}P_{15}M_{10}$	Medium	at 0.5 B	150	10
31	$M_bP_{15}M_{10}$	Medium	at B	150	10
32	$L_SP_{15}M_{10}$	Loose	at surface	150	10

PC. In this system, the data transferred to the indicator is transferred to the PC as it is via the indicator.

ARH-A waterproof, low capacity acceleration transducer (ARH-500A) was used. It is installed in water or ground or embedded in concrete. The rigid waterproof structure makes this transducer suitable for use in an adverse environment or for outdoor use.

5. Testing program

The testing program consists with a total number of tests of 32. Tests were performed in medium and loose soil state. Two bearing plate sizes, 100 mm or 150 mm were used and the models were tested at the surface of the soil and at a depth of 0.5B, B, and 2B where B is the diameter of the bearing plate as shown in Fig. 3. The impact load is applied by dropping the mass of 5 kg or 10 kg from a height of 500 mm. The details of abbreviation for the tested samples as well as example of models naming are explained in Table 3.

6. Testing procedure

The following steps describe the testing methodology:

1. Preparing the layers of sand which have a total depth of 400 mm (100 mm for each) as mentioned before depending on the required relative density.

2. Installing the accelerometers at the center of the sand layer in the vertical direction under the centroid of the bearing plate at a depth of (B) or (2B) according to the size of bearing plate.

Fig. 4 Small FWD main body KFD-100A

3. Installing the accelerometer in the horizontal direction near the surface at a depth of (10 mm).

4. Leveling the surface and installing the FWD at the center of the model surface and checking if it is perpendicular to the surface of the model.

5. Adjusting the data logger reader and the exclusive indicator TC-351F of the FWD to get zero readings.

6. Releasing the striking mass and the resulted response will be recorded and presented on a PC.

Fig. 4 shows a schematic diagram showing the longitudinal section of set-up of the physical model, and showing the location of transducers used.

7. Test results of dry medium and loose sandy soil under impact

Plots of the experiment results are presented in Figs. 7 to 10 for medium sand and 11 to (14) for loose sand.

Examinations of these figures show the behavior presented here after:

1. The impact load-time history is also of a single pulse but has no ideal sine shape. In case of medium sand, it almost vanishes or becomes of negligible value at the end of the impulse-time history when the impact plate is embedded at large depths while it ends at a magnitude equals or near to the magnitude of the weight of the falling hammer when the footing is placed at the top surface or embedded at a shallow depth.

2. When the impact load acts on a footing resting on loose sand, the impulse force-time history ends at values near to the weight of the falling hammer irrespective of other parameters (magnitude of the hammer weight or the footing diameter).

This tendency ensures the idea that, no reflection of the impulsive wave from the far boundaries is encountered (for both medium and loose sands), so that, the boundaries act as a free support (at the base) having no or negligible stiffness.

7.1 Amplitude of the impact force

Results of impact force-time history are plotted and shown in part "*a*" of each plot. Examining the figures reveals that:

Decreasing as the density of supporting medium (soil) decreases. The lowest amplitudes of the impulsive wave are found to be in models of loose soil for all cases of impact plate diameter, weight of the falling mass and height of fall of the hammer. In case of 100 mm diameter of impact plate, the reduction in impulse force amplitude from dense to loose sand ranges between 60%-70% (keeping other parameters unchanged) while in case of 150 mm impact plate, the reduction is about 45%-55%. This tendency is a common behavior of impulsive force amplitude magnitude since the magnitude of impulse is stiffness dependent. Stiffer soils tend to act as solids with high rebound capability. The same results were found by Al-Ameri (2014).

As the impact plate diameter increases, the magnitude of the impulsive amplitude increases also by about 30-40% in case of medium sand and by about 50-60% in case of loose soil. This tendency is attributed to the fact that the soil stiffness is related to two factors, degree of confinement which

increases with the footing area and the magnitude of the excited mass which depends, also upon the footing area.

As the energy of impact increases (due to an increase in the weight of the falling hammer), the amplitude of the impact increases also. A 100% increase in the weight results in an increase in the impulse amplitude by about 55-80% in case of medium sand and by about 45-55% in case of loose sand. This tendency is related to the fact that the impulse amplitude is energy dependent. The energy, meanwhile, decreases as the density also decreases that is, looser soils contribute more in energy dissipation though the magnitude of dissipation is less than the increase associated with the mass of falling hammer.

7.2 Response of soil beneath the footing

Figures of soil-foundation response show that:

1. The maximum response occurs either at the end of impulse time interval or within the free vibration phase (after vanishing of impulse). This behavior could be justified to the fact that the frequency ratio (β) (which is equal to ($\overline{\omega}/\omega$) that is, frequency of applied load to the natural frequency of the foundation soil system) becomes more than 1.0. Since ($\overline{\omega}$) is almost unchanged or its variation is minor; therefore, ω might be decreasing as the soil becomes more loose. Such a justification should follow that the stiffness reduces in large magnitudes as the soil density reduces. This might be a reasonable justification which will be highlighted in the following chapter. Such a tendency results in lower natural frequency of the soil-foundation system and therefore, $\overline{\omega}$ will be larger and hence β becomes larger than unity.

2. An important note can be highlighted from the plots, that is, higher displacement response is found to occur when the impact plate (footing) is placed at the top surface of the supporting soil (medium or loose). As the footing becomes deeper, the displacement response decreases down to a depth equals to twice the footing width (2B). This can be justified according to the degree of compaction of soil and hence, the excited soil mass during impact; that is, as the soil becomes looser, the excited mass reduces significantly while for deeper footing, the soil is naturally compacted and the excited mass starts to increase and the soil becomes more stiff.

These results are compatible with the findings of Al-Homoud and Al-Maaitah (1996) found that for forced vibration tests, there is an increase in natural frequency and a reduction in amplitude with the increase in embedment depth. The results are also in a greement with those of Mandal and Roychowdhury (2008) who presented the central response of the square raft under the step loading of 100 kN for different depth to width ratios. It was observed that the increase in the depth of embedment yields response of lesser amplitude and higher frequency.

3. One more notice is also recorded, that is, at the end of the impulsive-time period, the soil particles; still possess both velocity and acceleration in most cases. This behavior can result in higher responses (displacements) during the free vibration phase. This tendency was concluded earlier at this paragraph.

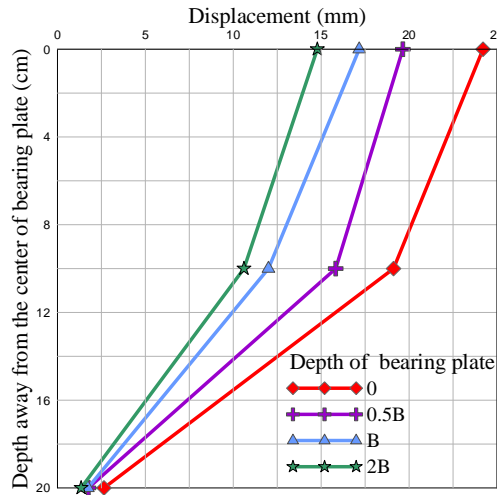### 7.3 Response inside the soil medium

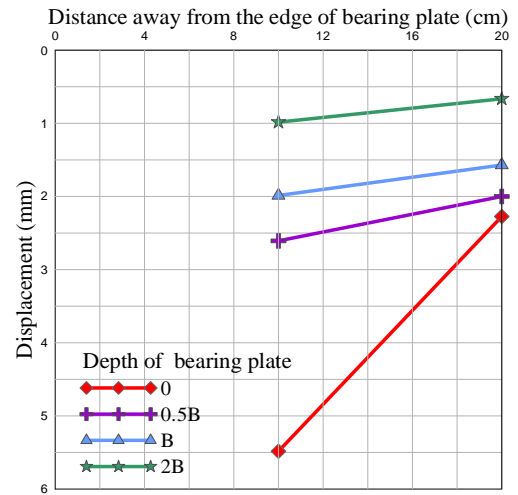(a) force-time history with displacement-time history

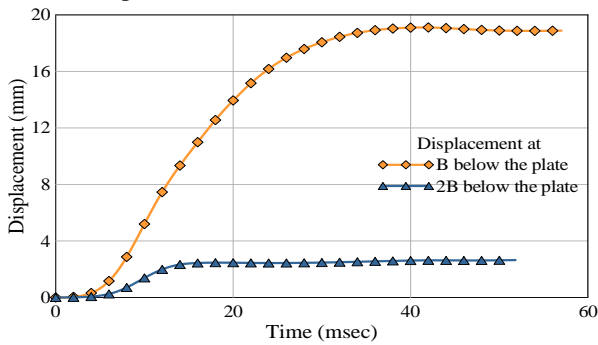(b) acceleration-time history

(c) velocity time-history
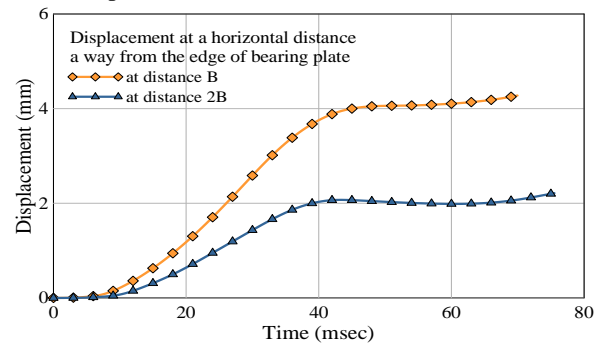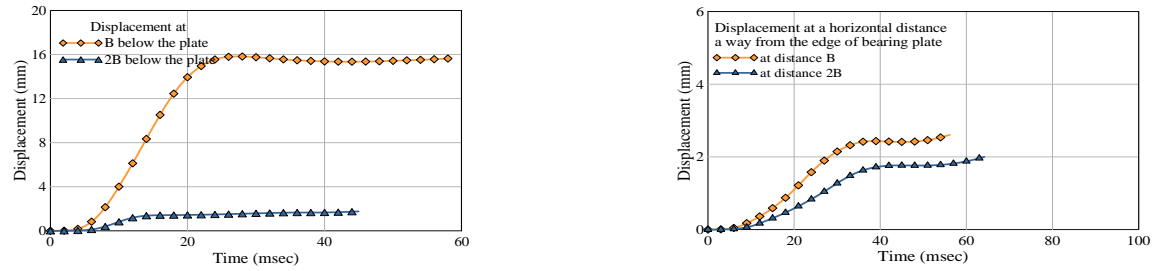

(d) displacement variation in vertical direction

(e) displacement variation in horizontal direction
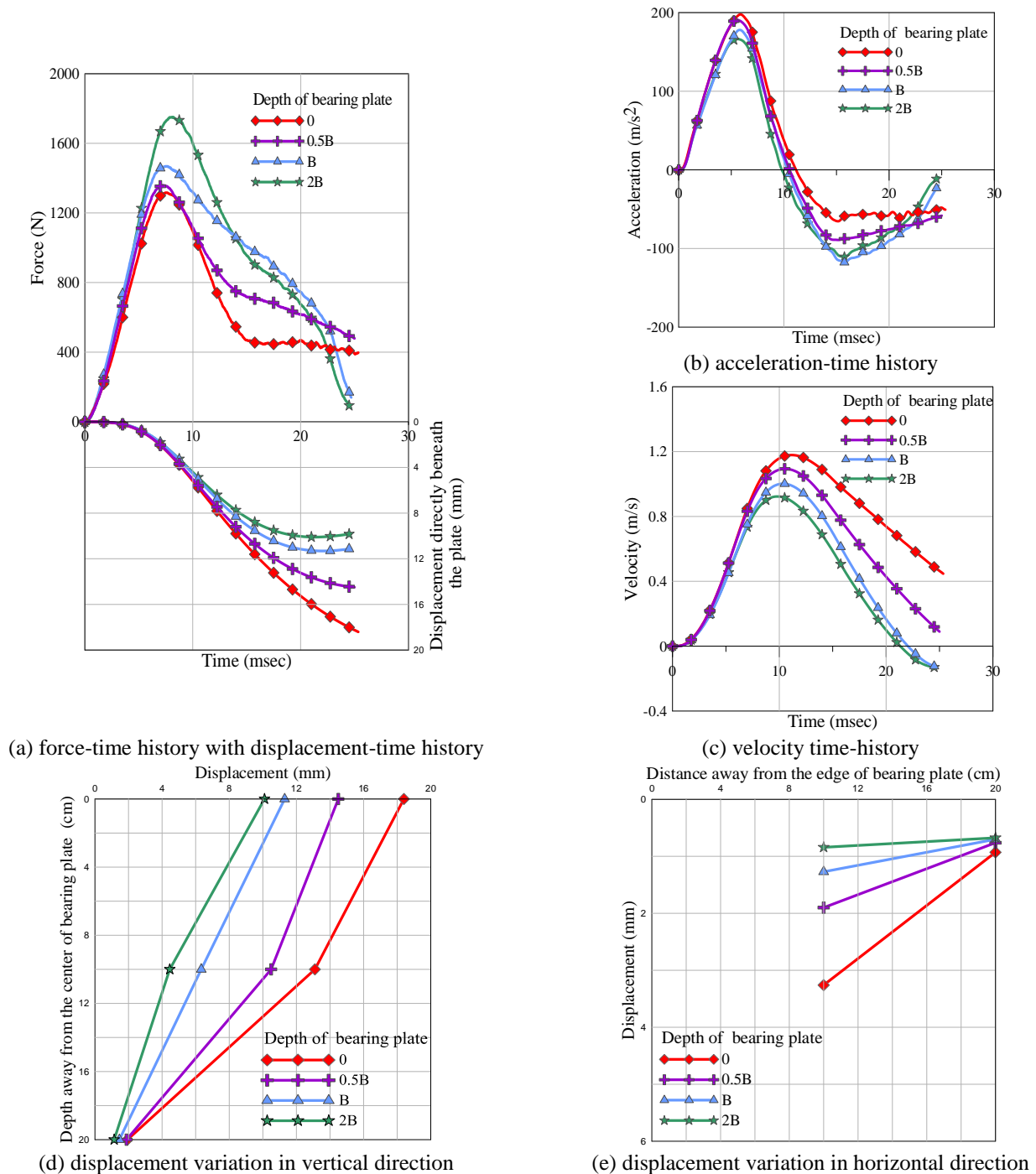
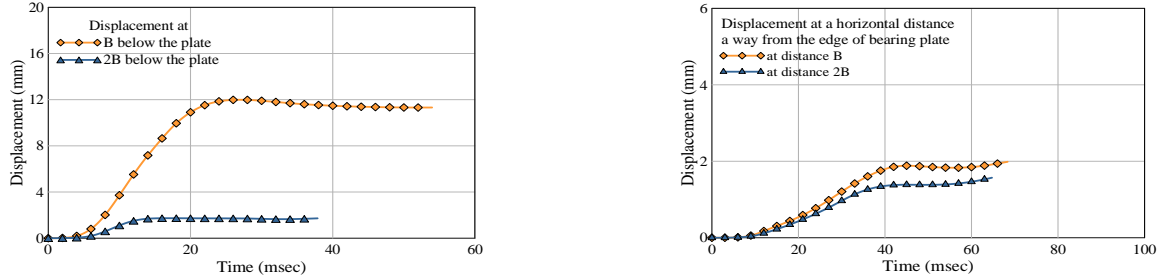Fig. 5 Test results for $MP_{10}M_5$ model

Four accelerometers (ARH-500A) were installed inside the soil to measure acceleration response under the impact load. Two accelerometers were installed at the center of the sand layer in the vertical direction under the centroid of the bearing plate at depths of (B) and (2B) according to the size of the bearing plate, and the other two accelerometers were installed in the horizontal direction at a depth of 10 mm at a distance of (B) and (2B) from the edge of the bearing plate.

From the obtained acceleration, processing software was used to carry out FFT to get the velocity and displacement. The maximum amplitudes of displacement of the response of these points in the vertical and horizontal directions were presented

to make a comparison of displacement inside the soil under the effect of impact load, and to clarify the response of the soil in the vertical and horizontal directions.

In general, at a certain distance in the vertical or horizontal direction within the soil medium as shown in parts *d*, *e*, *f*, *g*, *h*, and *i* of Figs. 5 to 12, it can be seen that the displacement increases with the increase of the amplitude of load in all directions.

the vertical displacements within the soil medium are found to decrease with depth and follow the conventional Bousinesq equation, which is, following different paths, therefore they reduce with depth. This tendency is related to
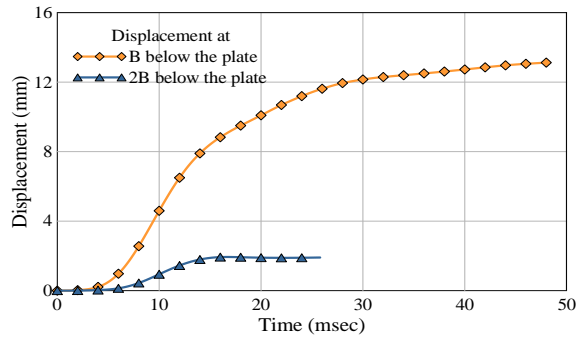
(f) The bearing plate at surface
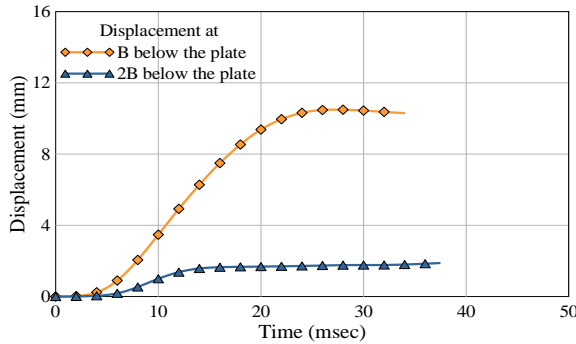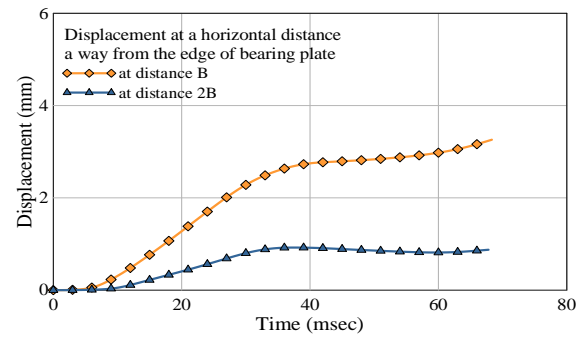
(g) The bearing plate embedded at 0.5 B depth
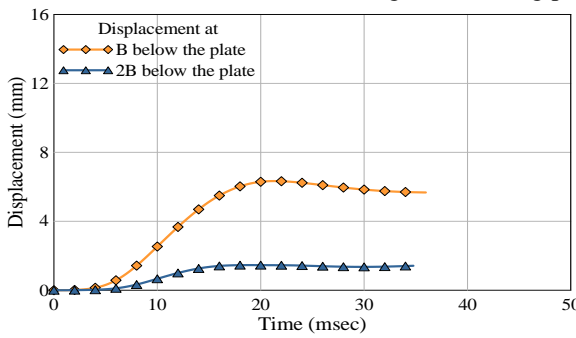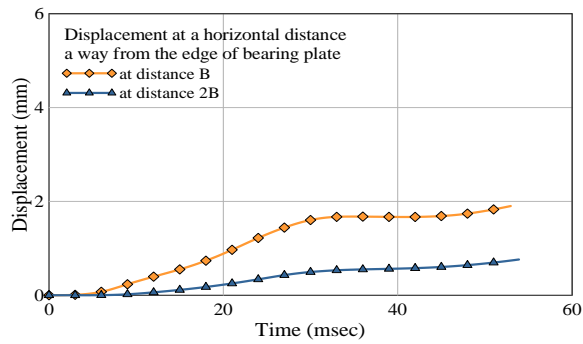
(h) The bearing plate embedded at B depth
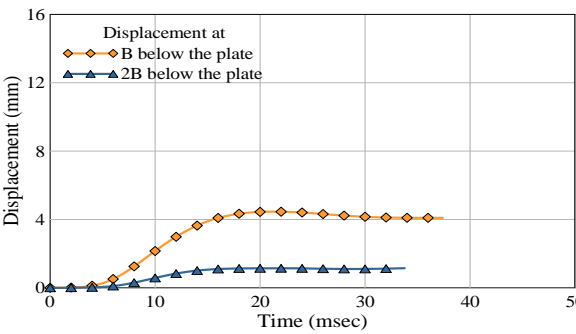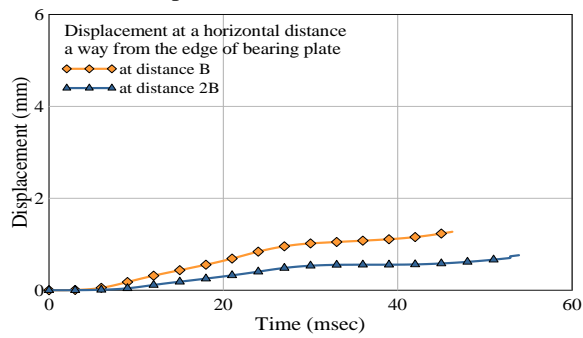
(i) The bearing plate embedded at 2B depth
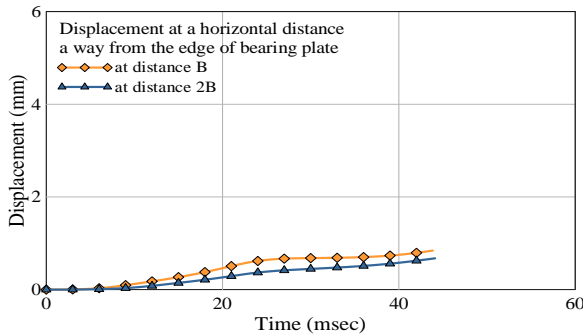
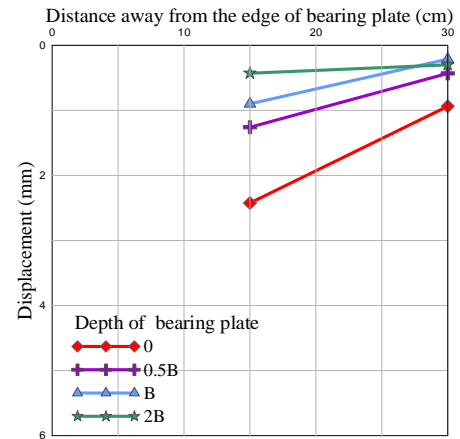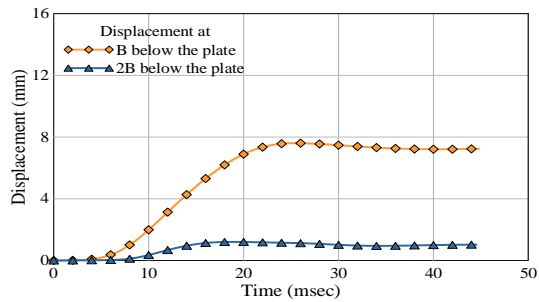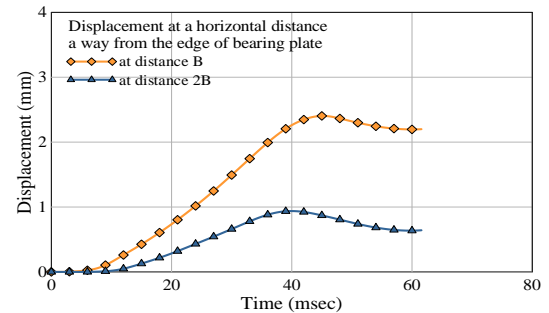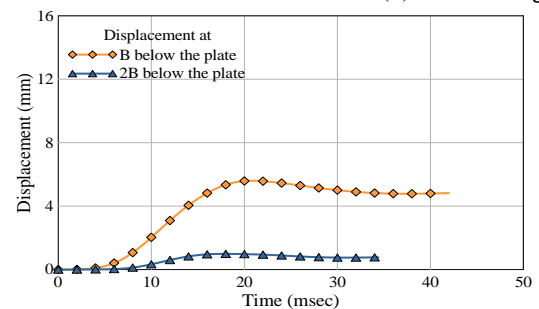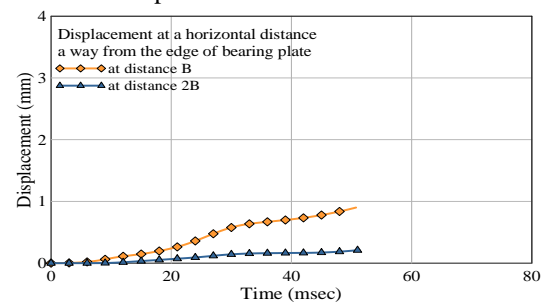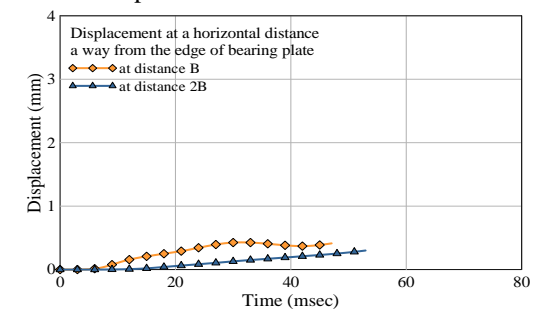Fig. 5 Continued

the larger void ratio which increases according to the results in unpredictable mechanisms of soil particles during impulse wave propagation. Ultimately, the responses were noted to vanish at depths below the footing especially at a depth equals to 2B by about 85-90% reduction in displacement caused by the impact load. As shown in parts (*d*, *e*, *f*, *g*, *h*, and *i*) from Figs. 5 to 12, there are common trends associated with impact for both cases (displacement in vertical and horizontal directions inside the soil medium) for both medium and loose

sand, these are:

a. In case of loose and medium sand, the reduction in the vertical displacement inside the soil medium at a depth B was about 30-55% for medium sand and 25-30% for loose sand and that when the plate diameter is 100 mm and falling mass 5 kg from a height of 500 mm. When the falling weight is increased 50% (falling mass 10 kg from a height of 500 mm), the reduction will be about 20-30% for medium sand and by about 10-13% for loose sand, but when the area of bearing
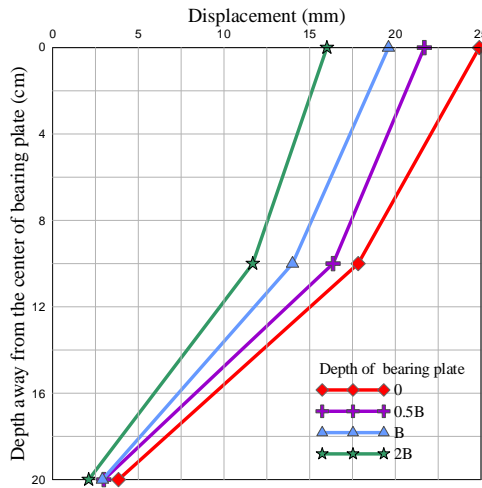
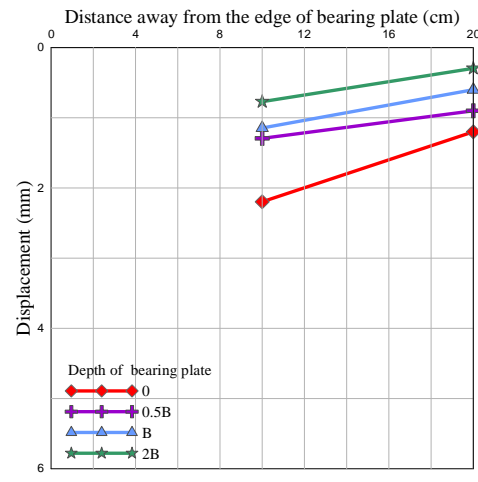(a) force-time history with displacement-time history
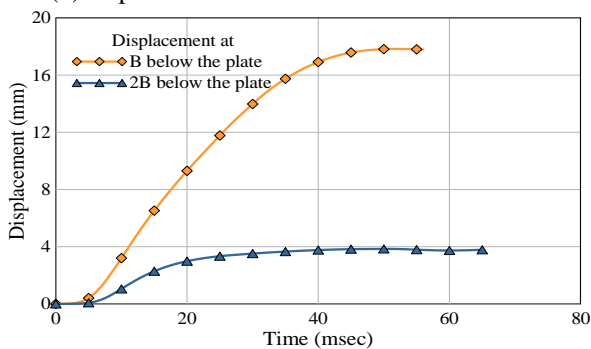

(b) acceleration-time history

(c) velocity time-history

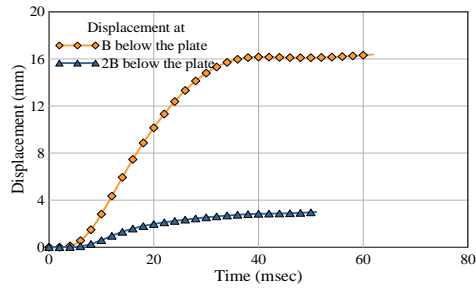(d) displacement variation in vertical direction

(e) displacement variation in horizontal direction
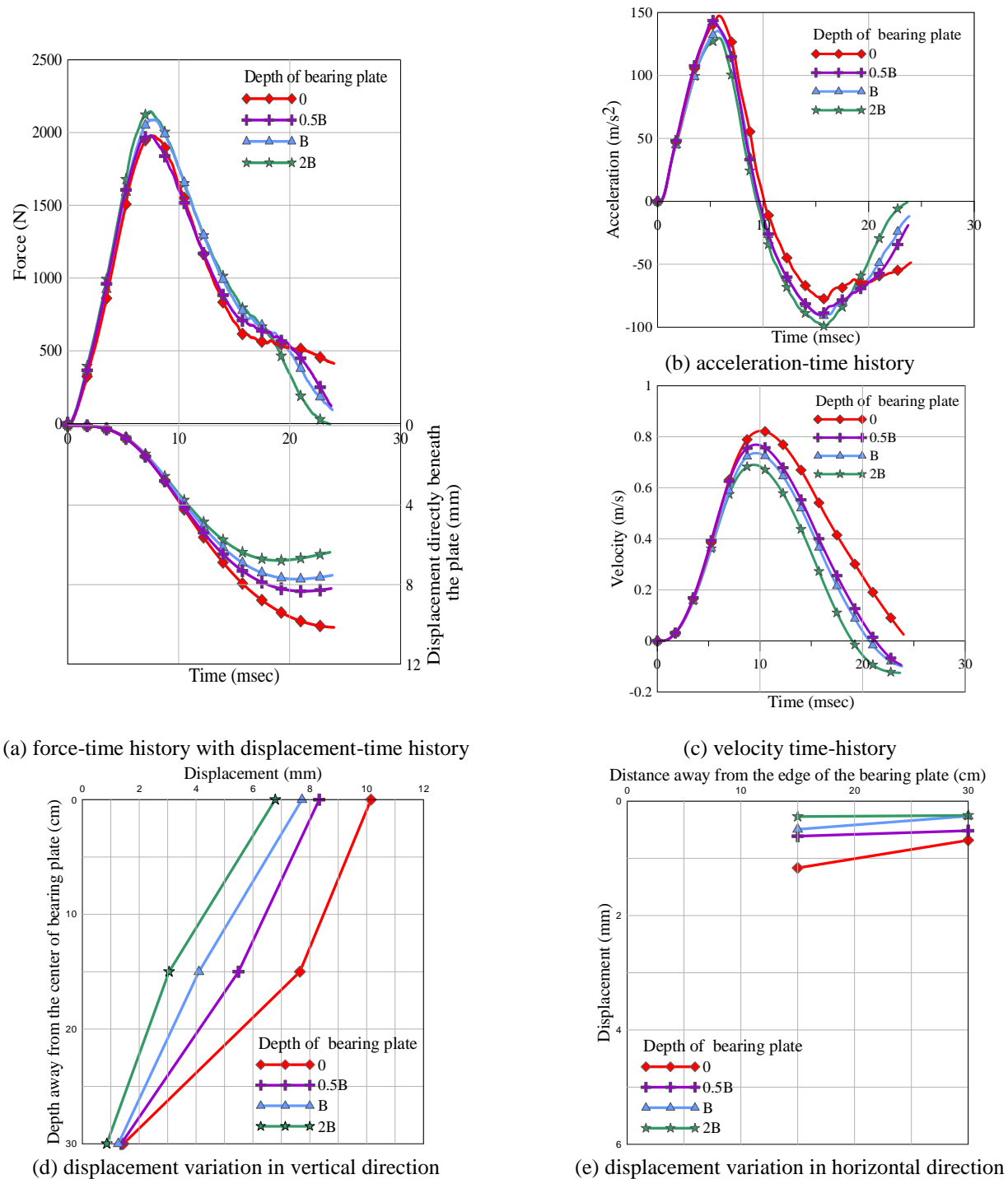
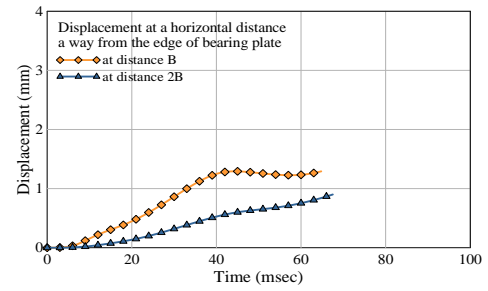Fig. 6 Test results for MP$_{15}$M$_5$ model

plate increases to about 125 % for the same force energy, the reduction will be about 35-45% and 25-40% for medium and loose sand, respectively (as shown in parts d of each figure). It is important to notice that the reduction in vertical direction in dense soil was higher than the reduction in loose and medium soil and it is about 50% and that is due to the fact that the void ratio of dense soil is smaller than in medium or loose sand.

b. In general, the reduction in displacement in the horizontal direction at a distance *B* away from the edge of the bearing plate was of negligible values (10% of the maximum response when the plate is at the surface and 5% when the

plate is embedded in the soil).

c. It can be seen from parts *e*, *f*, *g*, and h from each figure, that there is a time lag between the displacement in the vertical direction and the horizontal direction, and that is because the *P*-waves are the fastest, they will arrive first, followed by the *S*-waves.

8. Conclusions

1. The amplitude of the force-time history for dense soil
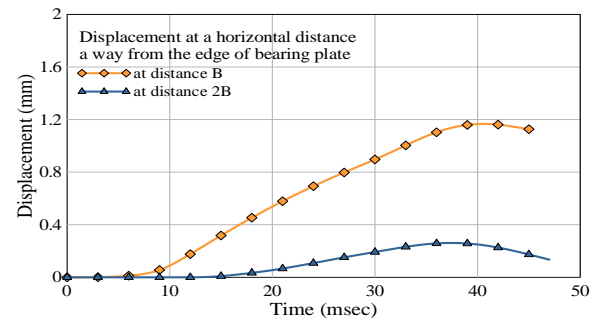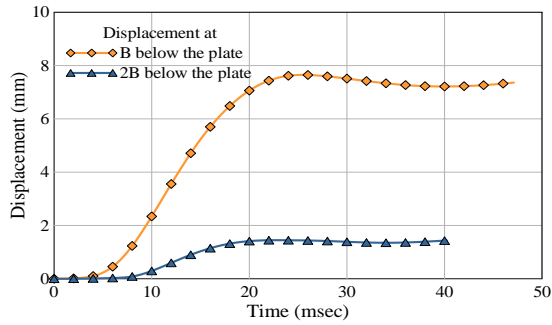
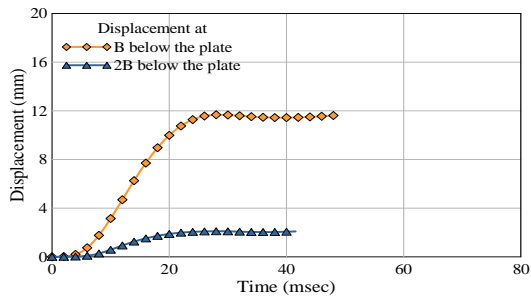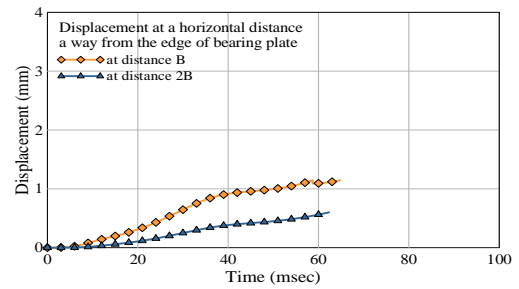(f) The bearing plate at surface
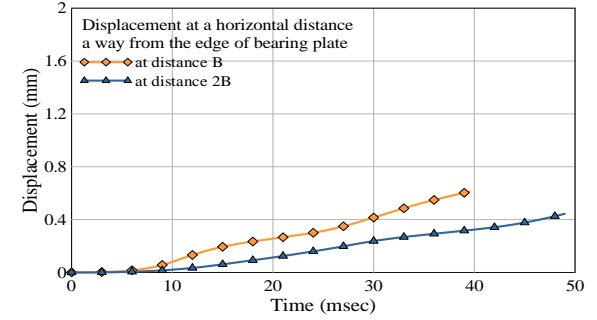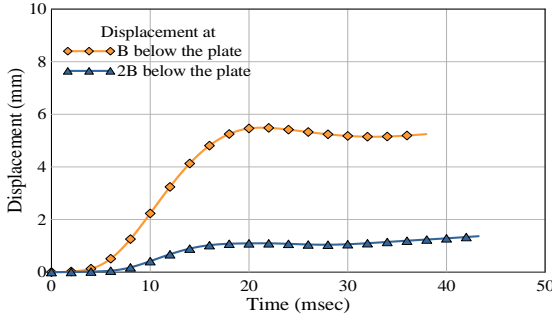
(g) The bearing plate embedded at 0.5 B depth
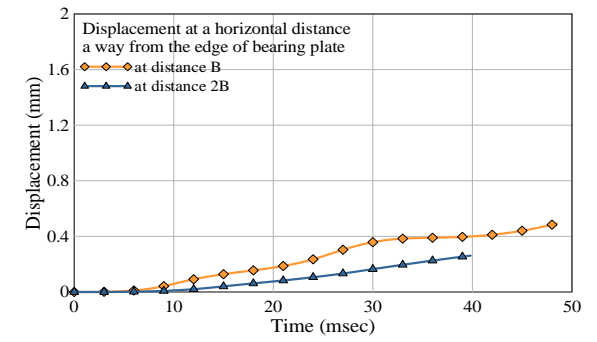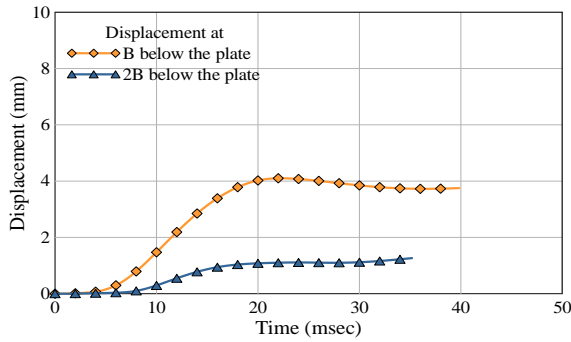
(h) The bearing plate embedded at B depth
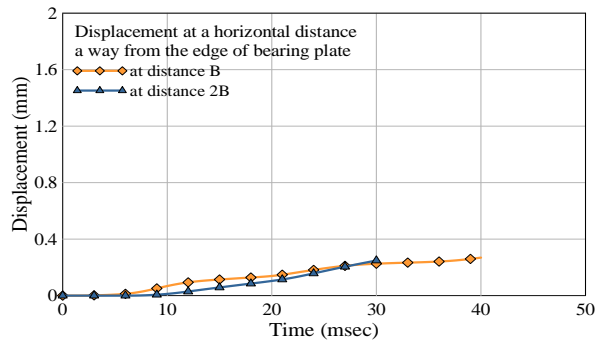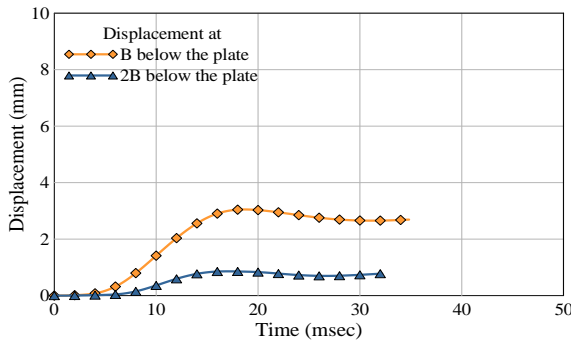
(i) The bearing plate embedded at 2B depth

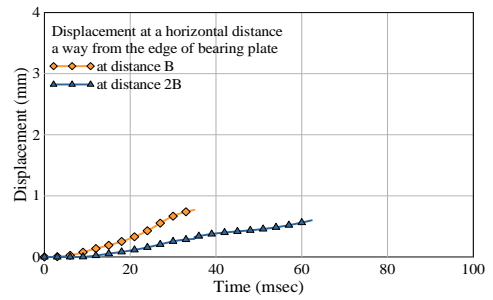Fig. 6 Continued

under impact load is harmonic with a single pulse, but has no ideal sine shape. The impulse almost vanishes or becomes of negligible value at the end of the impulse-time history in case of medium sandy soils while it ends at a magnitude equals or near to the magnitude of the weight of the falling hammer in case of sand of loose density.

2. Increasing footing embedment depth results in the followings:

a. Amplitude of the force-time history increases by about 10-30%. due to increase in the degree of confinement with the increasing in the embedment.

b. The displacement response of the soil will decreases by about 25-35% for loose sand, 35-40% for medium sanddue to increase in the overburden pressure when the embedment depth increased and that lead to increasing in the stiffness of the sandy soil.

3. When the area of the bearing plate (footing) is increased by 125%, the following points are obtained:

a. The amplitude of the force-time history will be increased. It will increase by about 50-60% for loose
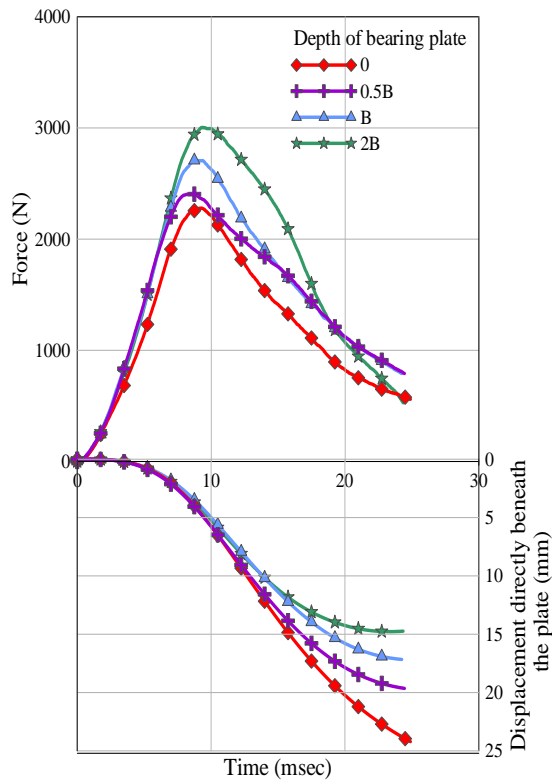
(a) force-time history with displacement-time history
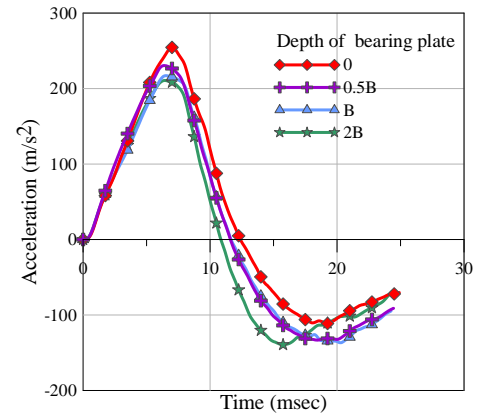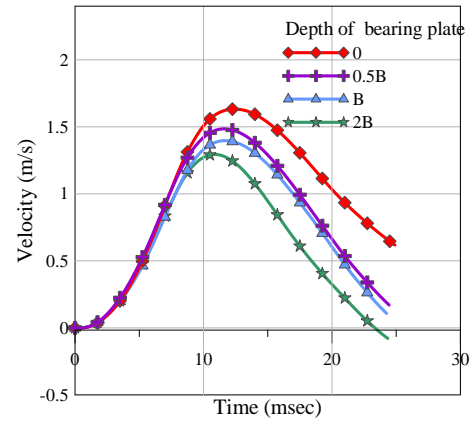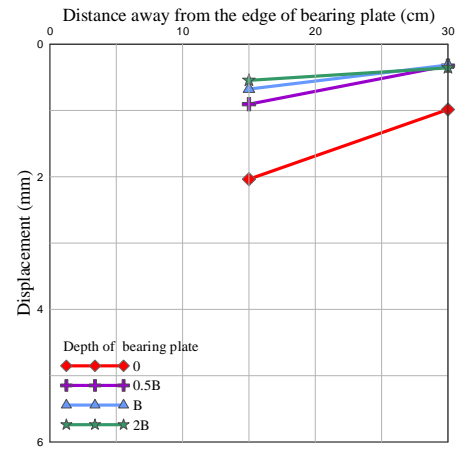
(b) acceleration-time history

(c) velocity time-history

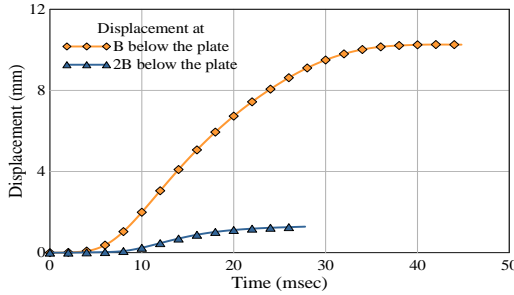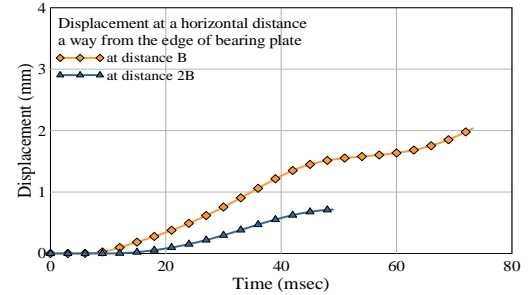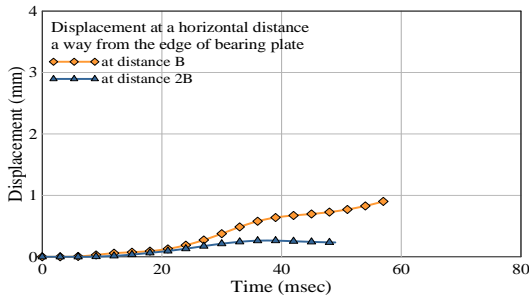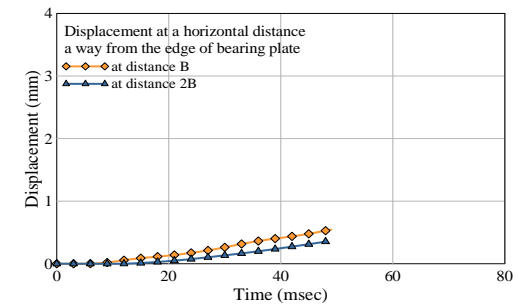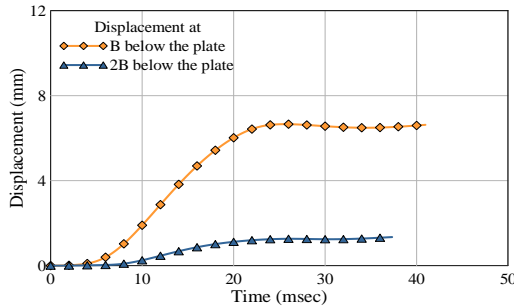(d) displacement variation in vertical direction

(e) displacement variation in horizontal direction

(f) The bearing plate at surface

Fig. 7 Test results for $MP_{10}M_{10}$ model
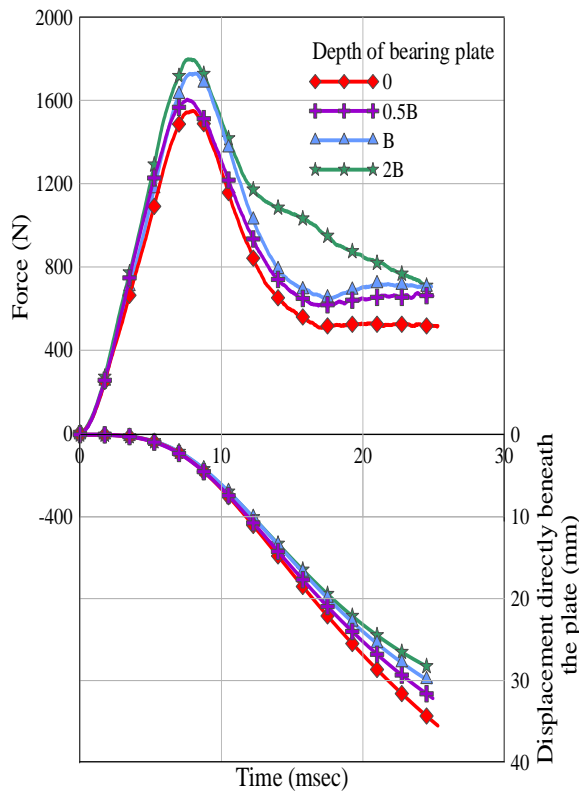
(g) The bearing plate embedded at 0.5 B depth
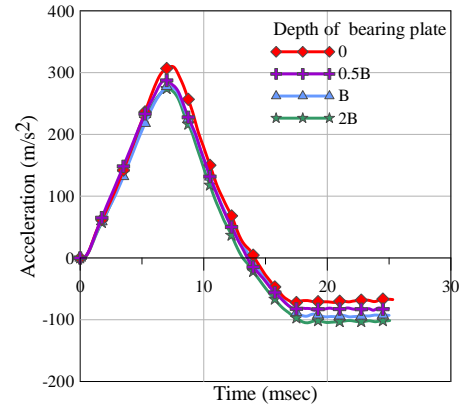

(h) The bearing plate embedded at B depth
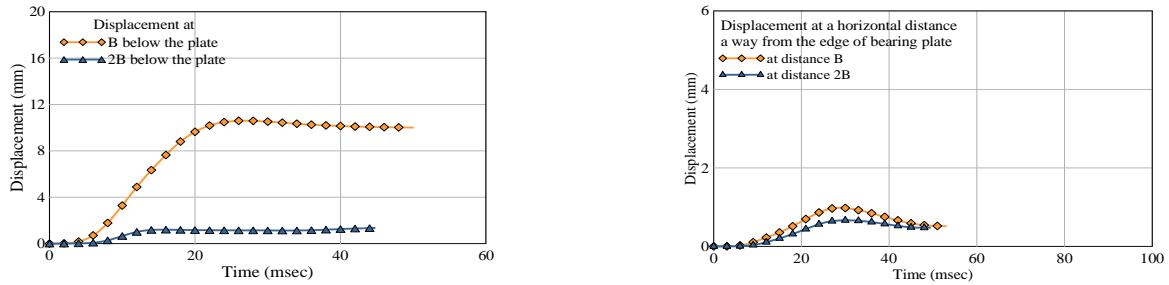
(i) The bearing plate embedded at 2B depth
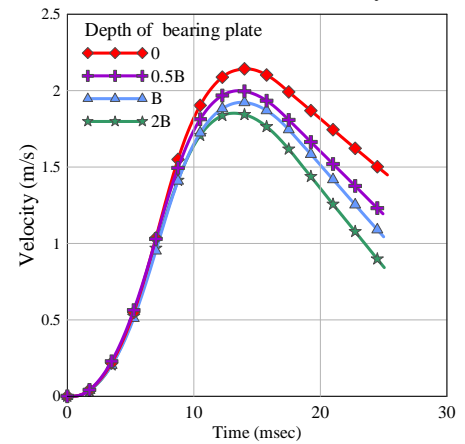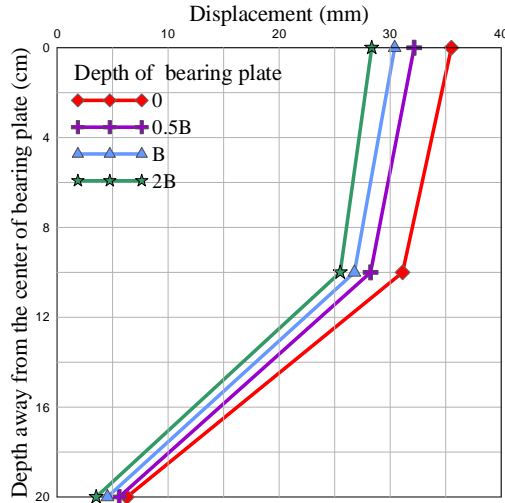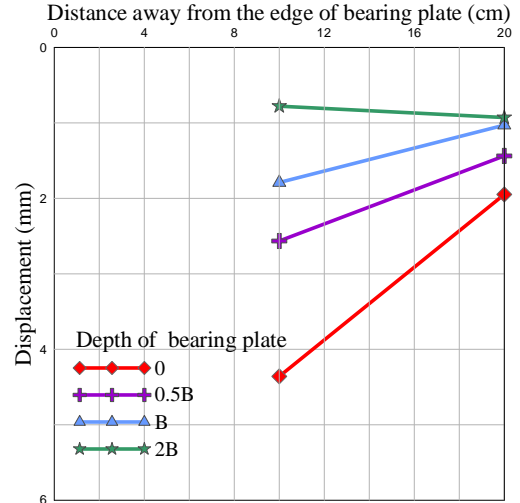
Fig. 7 Continued

(a) force-time history with displacement-time history

(b) acceleration-time history
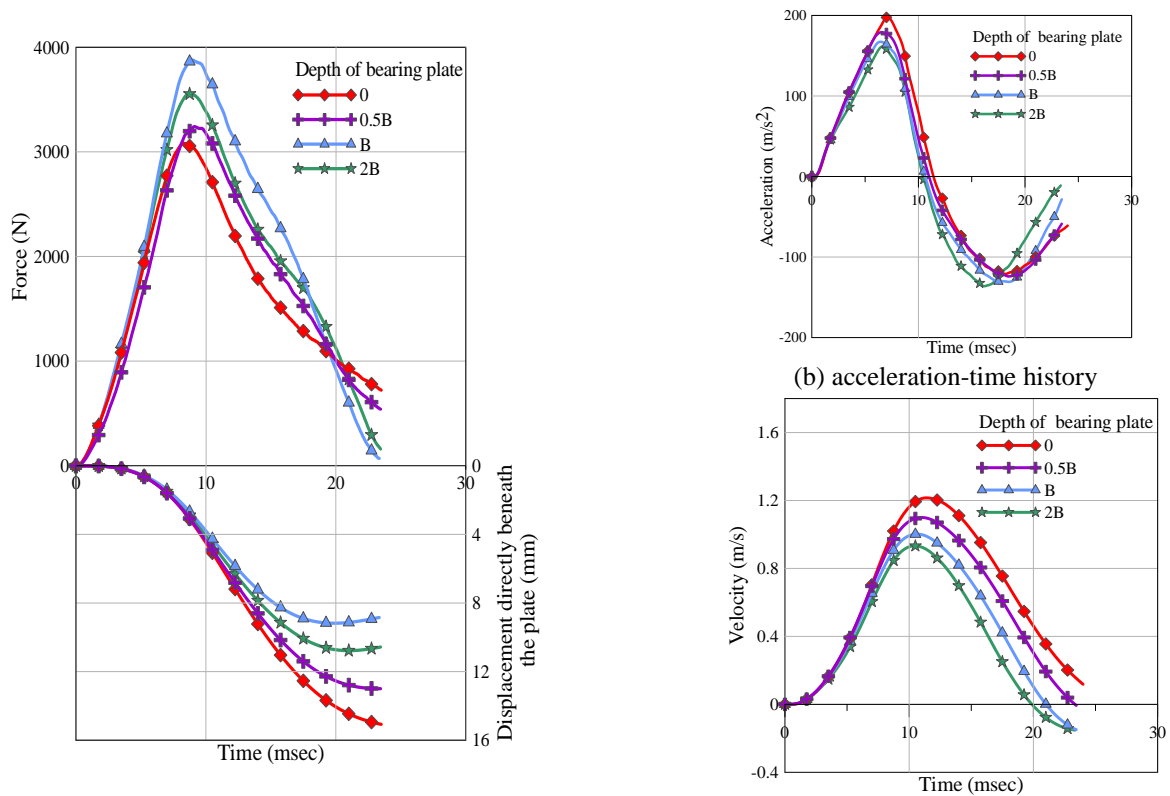
(c) velocity time-history

Fig. 8 Test results for $MP_{15}M_{10}$ model
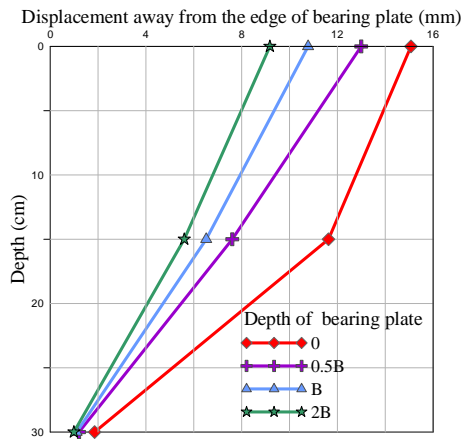
(d) displacement variation in vertical direction

(e) displacement variation in horizontal direction
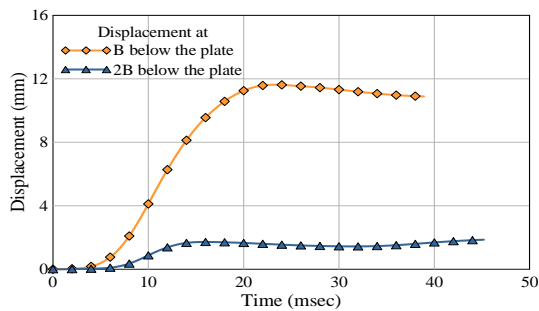
(f) The bearing plate at surface

(g) The bearing plate embedded at 0.5 B depth
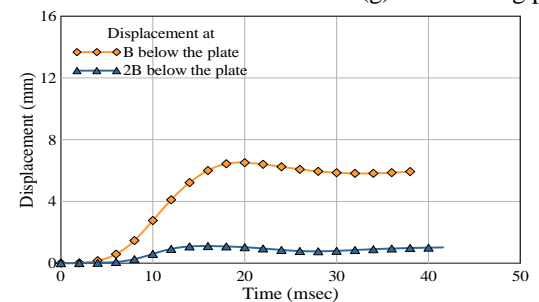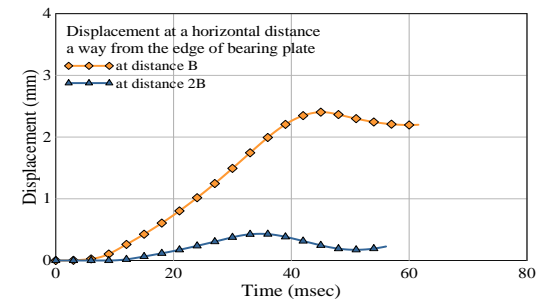
(h) The bearing plate embedded at B depth

(i) The bearing plate embedded at 2B depth

Fig. 8 Continued
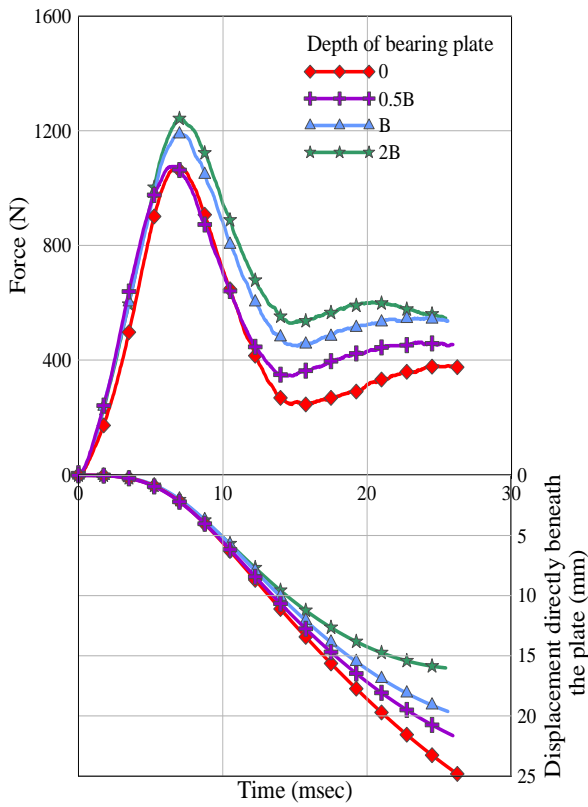
(a) force-time history with displacement-time history
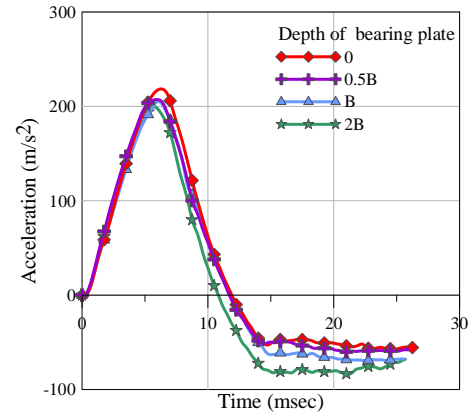
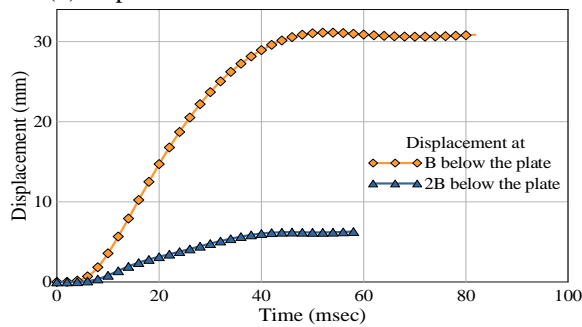(b) acceleration-time history
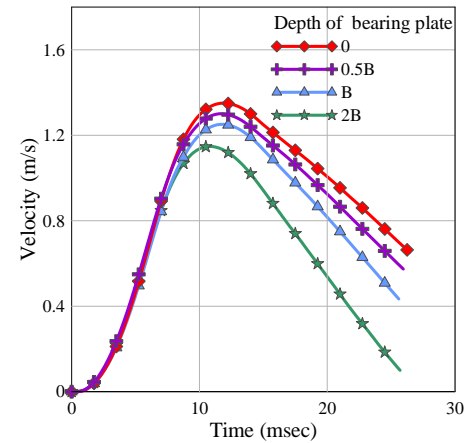
(c) velocity time-history

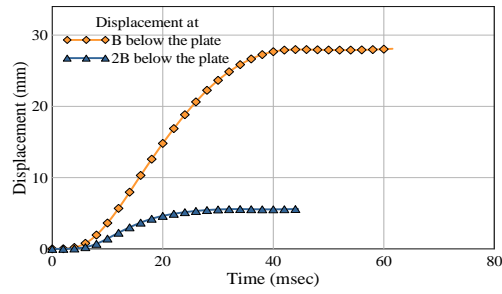(d) displacement variation in vertical direction

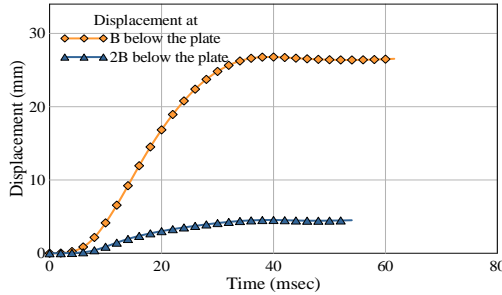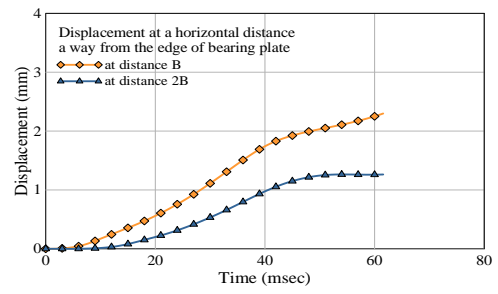(e) displacement variation in horizontal direction

(f) The bearing plate at surface

Fig. 9 Test results for $LP_{10}M_5$ model

(g) The bearing plate embedded at 0.5 B depth
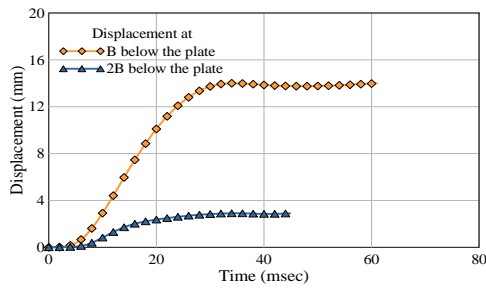
(h) The bearing plate embedded at B depth

(i) The bearing plate embedded at 2B depth

Fig. 9 Continued
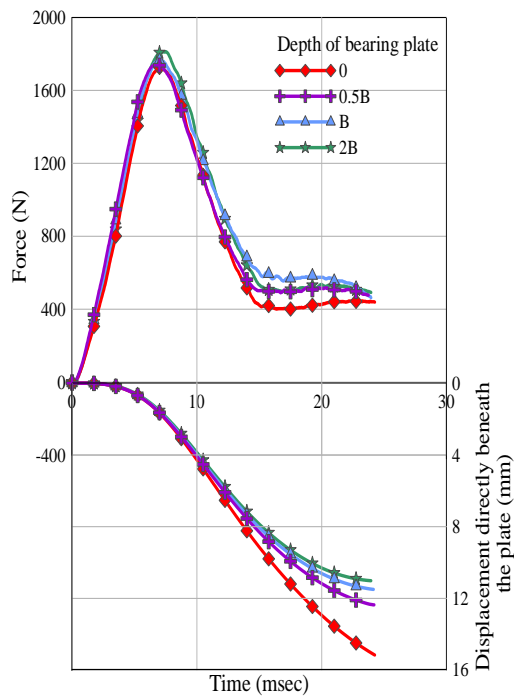
(a) force-time history with displacement-time history
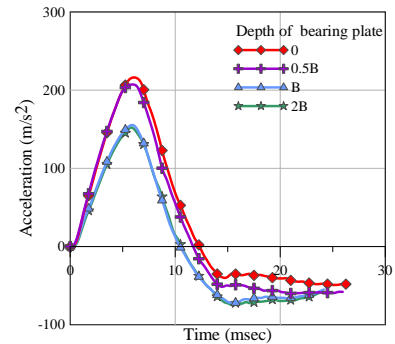
(b) acceleration-time history
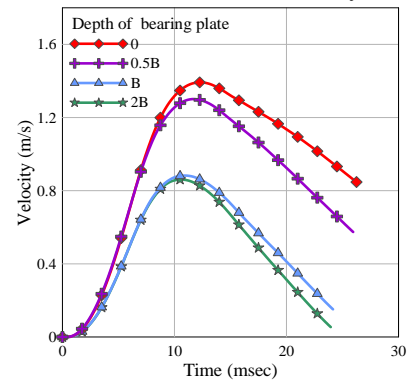
(c) velocity time-history

Fig. 10 Test results for $LP_{15}M_5$ model
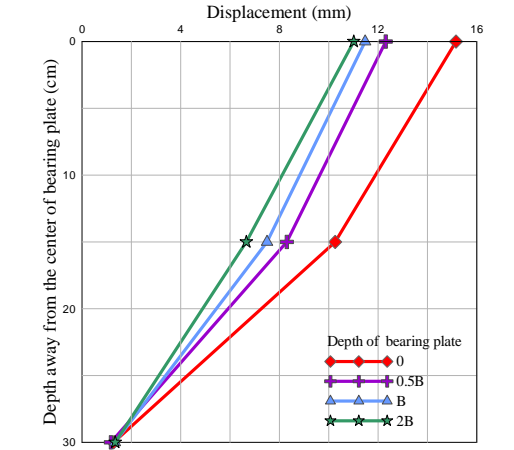
(d) displacement variation in vertical direction   (e) displacement variation in horizontal direction
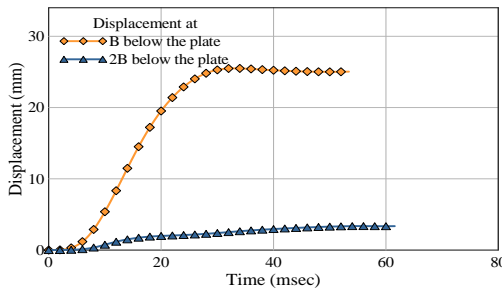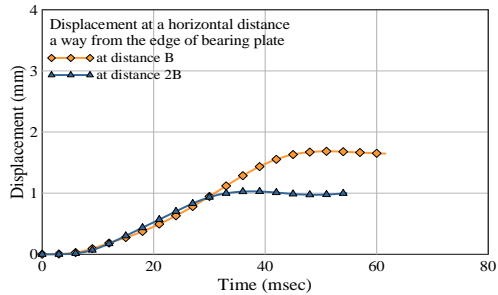
(f) The bearing plate at surface

(g) The bearing plate embedded at 0.5 B depth
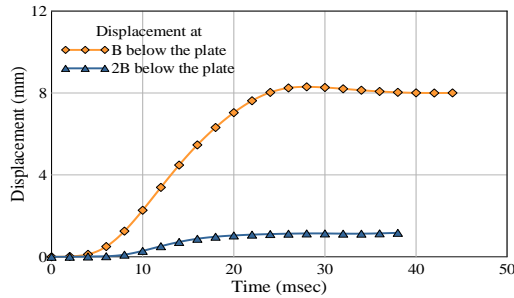
(h) The bearing plate embedded at B depth

(i) The bearing plate embedded at 2B depth

Fig. 10 Continued

(a) force-time history with displacement-time history

(b) acceleration-time history

(c) velocity time-history

(d) displacement variation in vertical direction

(e) displacement variation in horizontal direction

(f) The bearing plate at surface

Fig. 11 Test results forLP$_{10}$M$_{10}$ model

(g) The bearing plate embedded at 0.5 B depth

(h) The bearing plate embedded at B depth
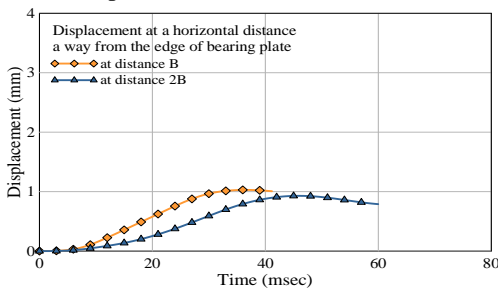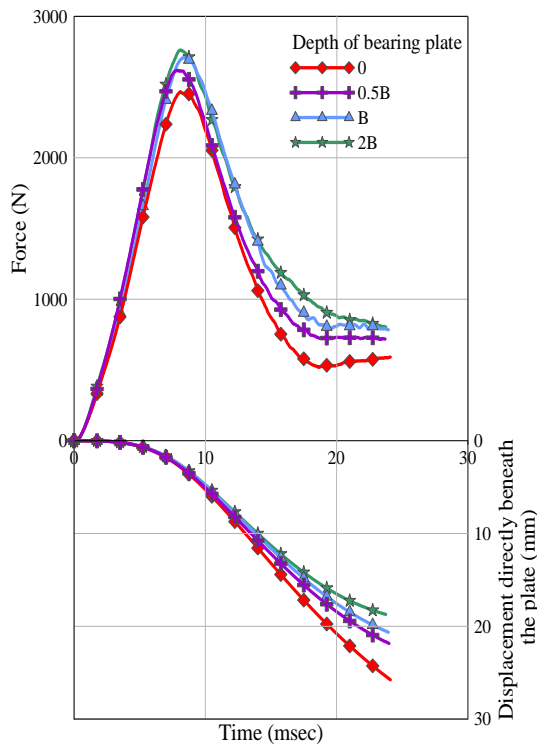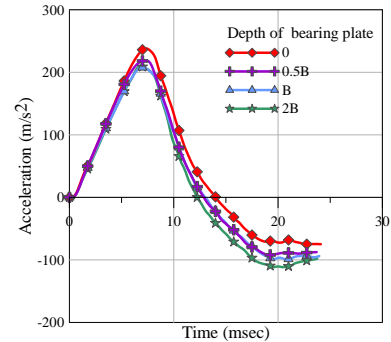

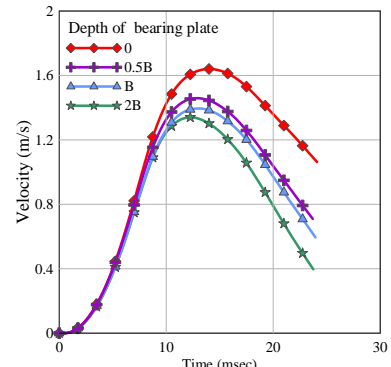(i) The bearing plate embedded at 2B depth

Fig. 11 Continued
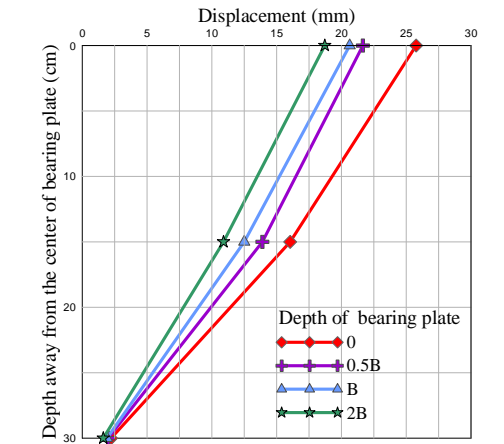

(a) force-time history with displacement-time history
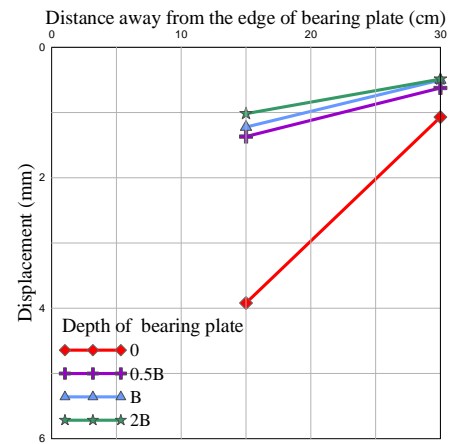
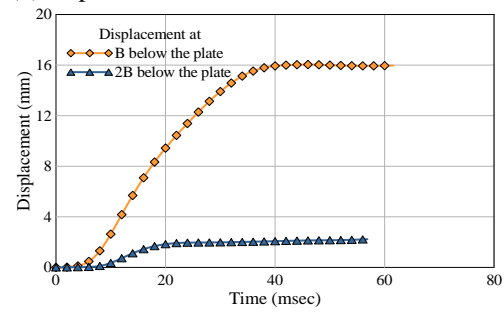(b) acceleration-time history

(c) velocity time-history

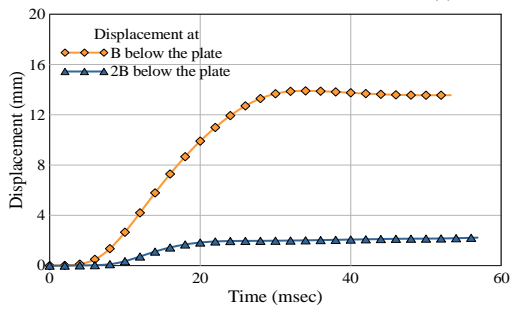Fig. 12 Test results for LP$_{15}$M$_{10}$ model
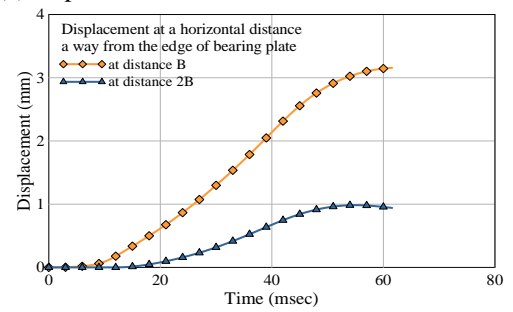
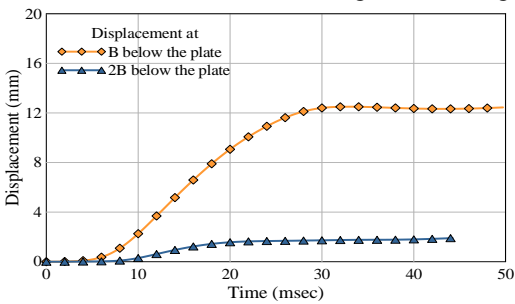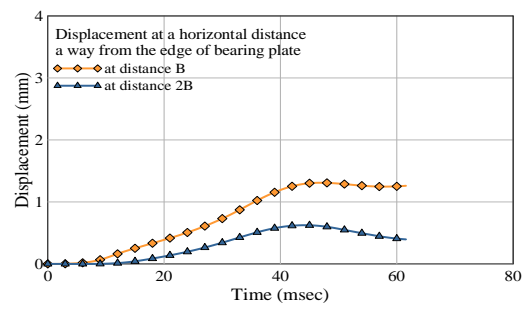(d) displacement variation in vertical direction

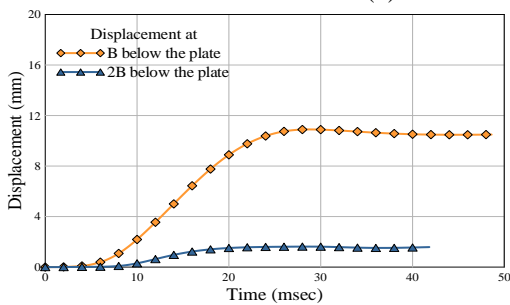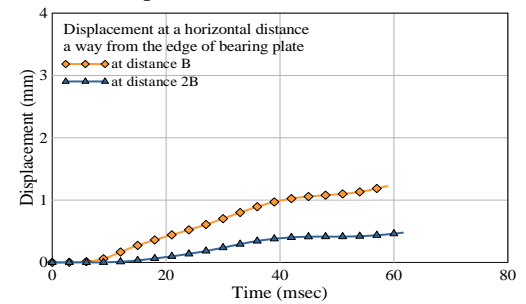(e) displacement variation in horizontal direction

(f) The bearing plate at surface

(g) The bearing plate embedded at 0.5 B depth

(h) The bearing plate embedded at B depth
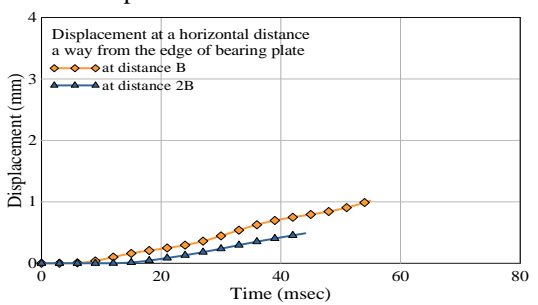
(i) The bearing plate embedded at 2B depth

Fig. 12 Continued

sand, and 30-40% for medium sand. This tendency is attributed to the fact that the soil stiffness is related to two factors, degree of confinement which increases with the footing area and the magnitude of the excited mass which depends, also upon the footing area.

b. The displacement response reduces in case of soil due to reduction in the stresses caused by the increase of contact area. The response reduces by about 30-45% for dry sand.

4. The displacement response (vertical and horizontal) always follow the same behavior (decreasing with depth irrespective of the depth of impact plate) as the behavior of static load (live loads or surcharge) with depth following the conventional Bousinesq equation.

References

Al-Ameri, A.F.I. (2014), "Transient and steady state response analysis of soil foundation system acted upon by vibration", Ph.D. Thesis, Civil Engineering Department, University of Baghdad, Iraq.

Al-Homoud, A.S. and Al-Maaitah, O.N. (1996), "An experimental investigation of vertical vibration of model footings on sand", *Soil Dyn. Earthq. Eng.*, **15**(7), 431-445.

American Society of Testing and Materials (ASTM) (1969), Standard Test Method for Relative Density of Cohesionless Soils, ASTM D 2049-69 International, West Conshohocken, Pennsylvania, USA.

American Society of Testing and Materials (ASTM) (1969), Standard Test Method for Relative Density of Cohesionless Soils, ASTM D 2049-69 International, West Conshohocken, Pennsylvania, USA.

American Society of Testing and Materials (ASTM) (2000), Standard Test Method for Minimum Index Density and Unit Weight of Soils and Calculation of Relative Density, ASTM D4254-00 International, West Conshohocken, Pennsylvania, USA.

American Society of Testing and Materials (ASTM) (2006), "Standard Test Method for Specific Gravity of Soil Solids by Water Pycnometer", ASTM D854, West Conshohocken, Pennsylvania, USA.

American Society of Testing and Materials (ASTM) (2006), Standard Test Method for Particle Size-Analysis of Soils, ASTM D422-02 (2002), West Conshohocken, Pennsylvania, USA.

Bhandari, P.K. and Sengupta, A. (2014), "Dynamic aAnalysis of machine foundation", *Int. J. Innov. Res. Sci. Eng. Technol.*, **3**(4), 169- 176.

Ergun, E., Yilmaz, Y. and Ç allioğlu, H. (2016), "Free vibration and buckling analysis of the impacted hybrid composite beams", *Struct. Eng. Mech.*, **59**(6), 1055-1070.

FatihKarahan, M.M. and Pakdemirli, M., (2017), "Vibration analysis of a beam on a nonlinear elastic foundation", *Struct. Eng. Mech.*, **62**(2), 171-178.

Fattah, M.Y., Al-Mosawi, M.J. and Al-Ameri, A.F.I. (2016), "Vibration response of saturated sand - foundation system", *Earthq. Struct.*, **11**(1), 83-107.

Fattah, M.Y., Salim, N.M. and Al-Shammary, W.T. (2015), "Effect of embedment depth on response of machine foundation on saturated sand", *Arab. J. Sci. Eng.*, **40**(11), 3075-3098.

Kim, Y.S., Miura, K., Miura, S. and Nishimura, M. (2001), "Vibration characteristics of rigid body placed on sand ground", *Soil Dyn. Earthq. Eng.*, **21**(1), 19-37.

Mandal, J.J. and Roychowdhury, S. (2008), "Response of rectangular raft foundations under transient loading", *Proceedings, 12th International Conference of International Association for Computer Methods and Advanced in Geomechanis (IACMAG)*, India, 524-530.

Prakash, S. and Puri, K.V. (2006), "Foundation for vibrating machines", *J. Struct. Eng.*, **33**(1), 13-29.

Svinkin, M.R. (2008), "Dynamic effects of impact machine foundations", *Geotechnical Earthquake Engineering and Soil Dynamics IV*, 1-17).

Turner, J.R. and Kulhawy, F.H. (1987), "Experimental analysis of drilled foundations subjected to repeated axial loads under drained conditions", Report EL-S32S, Electric Power Research Institute, Palo Alto, California.

CC